The impact of molecular weight on the segregative phase separation-induced molecular fractionation of aqueous gum Arabic/xanthan mixtures

Hu, B., Zhang, C., Han, L., Cao, J., Yang, J., Zheng, Q., Zhang, X., Liu, Y. and Yao, Z

International Journal of Biological Macromolecules 304 (2025) 140969

Contents lists available at ScienceDirect

International Journal of Biological Macromolecules

journal homepage: www.elsevier.com/locate/ijbiomac

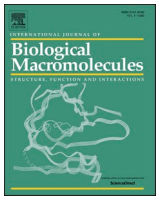

The impact of molecular weight on the segregative phase separation-induced molecular fractionation of aqueous gum Arabic/xanthan mixtures

Bing Hu [a,*], Cunzhi Zhang [a], Lingyu Han [a], Jijuan Cao [a,*], Jixin Yang [b], Qiuyue Zheng [a], Xiaobo Zhang [a], Yu Liu [a], Ziang Yao [a,*]

[a] Key Lab of Biotechnology and Bioresources Utilization of Ministry of Education, College of Life Science, Dalian Minzu University, Dalian, Liaoning 116600, China
[b] Faculty of Social and Life Sciences, Wrexham University, Plas Coch, Mold Road, Wrexham LL11 2AW, United Kingdom

ARTICLE INFO

Keywords:
Segregative phase separation
Molecular weight
Fractionation
Gum Arabic
Xanthan

ABSTRACT

Segregative phase separation of natural polymers has drawn significant research interest because of its diverse applications in the food industry. However, there is limited research on how molecular weight (Mw) influences segregative phase separation. This study aims to investigate the impact of Mw on segregative phase separation-induced molecular fractionation in mixed gum Arabic/Xanthan (GA/XG) solutions. The analysis focused on a single type of gum Arabic (referred to as EM10), with the molecular weights of both solid and liquid xanthan gum (XG) samples being altered through $^{60}Co_{\gamma}$ irradiation. These modified samples were evaluated using gel permeation chromatography combined with multi-angle laser light scattering (GPC-MALLS). The results demonstrated that the fractionation process of GA increased the content of the arabinogalactan-protein complex (AGP), increasing from an initial 29 % to a final 40 % within the GA/XG system (fixed with a mixture of 8 % EM10/0.8 % XG). When analyzing phase separation-induced molecular fractionation as a function of Mw, an increase in Mw (3.6×10^5–1.9×10^6) was associated with a corresponding rise in the degree of phase separation-induced fractionation. This was attributed to the irradiation-mediated breakage of XG chains. This study deeply analyzed the effect of Mw on the phase separation behavior and molecular fractionation mechanism of the GA/XG system. The results showed that when the Mw of XG was 3.6×10^5 (XG4) as a minimum, the AGP content was 29 % when mixed with GA, and when the Mw of XG was 1.9×10^6 (Control XG) as a maximum, the AGP content was 40 % when mixed with GA. The increase of Mw optimised the emulsion stabilisation property of GA significantly, which provided great practical value for its industrial applications.

1. Introduction

Phase separation is a common characteristic of aqueous biopolymer preparations. When a pair of biopolymers separates in a specific liquid phase, it can be classified as either segregative or associative phase separation [1,2]. The associative phase of the separation process involves the use of two suitable solvents, enabling the enrichment of the target biopolymers in one of the resulting phases, while the other phase predominantly contains the corresponding solvent [3,4]. This strategy is commonly used when preparing biopolymer mixtures with opposite charges. However, segregative phase separation is a phenomenon typically observed between mutually incompatible macromolecules, leading to the enrichment of specific molecules in each of the liquid phases [5]. Due to the opposing mechanisms involved in associative and segregative phase separations, most studies on mixed systems have focused exclusively on one of these forms under specific experimental conditions. As a result, it is often incorrectly assumed that these two types of phase separation cannot co-exist. However, Haug et al. demonstrated various phase separations in κ-carrageenan and fish gelatin systems by lowering the temperature. They observed the presence of emulsion-like composite condensed structures within the bicontinuous phase at low temperatures and low ionic strengths, providing evidence for the co-existence of associative and segregative phase separations [6]. Phase separation has been widely applied in industrial processes, including protein separation and purification [7], microencapsulation [8], improving emulsion stability [9], developing microstructures for food products, and various

* Corresponding authors.
E-mail addresses: hubing19871121@163.com (B. Hu), 20191414@dlnu.edu.cn (J. Cao), ziangyao@163.com (Z. Yao).

https://doi.org/10.1016/j.ijbiomac.2025.140969
Received 11 May 2024; Received in revised form 22 January 2025; Accepted 11 February 2025
Available online 11 February 2025

biomedical applications [10].

Gum Arabic (GA) is a natural gum derived from the hardened sap of acacia trees, composed of a complex mixture of glycoproteins and polysaccharides. It is commonly used in the food industry as a stabilizing agent [11]. GA is composed of three main fractions: the arabinogalactan-protein complex (AGP), arabinogalactan (AG), and glycoprotein (GP). The AGP fraction, which contains approximately 10 % protein, can have a molecular weight reaching several million Daltons and is known to play a significant role in emulsification [12].

The anionic polyelectrolyte xanthan gum (XG) has a high molar mass and is composed of a mixture of sodium, potassium, and calcium salts. Structurally, its backbone is formed by β-(1 → 4)-D-glucopyranosyl units, with a trisaccharide side chain attached to the C-3 position of every other unit. This side chain consists of one D-glucuronosyl unit between two D-mannosyl units, giving XG a pentameric structure. Functionally, XG is a biopolymer produced as a byproduct of microbial fermentation of starch-rich raw materials and is widely used in industrial applications as a suspension agent or thickener [13,14].

Natural polymers, including pectins and other marine-derived polysaccharides (such as chitin/chitosan, alginates, and carrageenans), predominantly undergo chain scission when exposed to irradiation, leading to significant decreases in their molecular weight [15]. This process is often accompanied by the formation of oxidation products and a reduction in crystallinity. The degradation of these polysaccharides enhances their suitability for various applications, including the production of healthcare products, cosmetic ingredients, plant growth promoters, and viscosity modifiers in the food and textile industries [16]. Although both enzymatic degradation and chemical modification can reduce the molecular weight of macromolecules, the rate and extent of reduction are difficult to control; therefore, irradiation was selected for XG degradation [17]. In degrading polymers, rapid recombination at the ends of broken chain is sterically hindered. Hence, because of disproportionation, polymer radicals are stabilized with the formation of two stable end groups resulting in reduced chain length, lower molecular weight polymers. While macromolecular structure plays a major role in determining the irradiation induced reactions, large differences in the extent of chain scission can also result from variations in processing conditions or post-irradiation conditions (temperature, dose rate, the presence of oxygen/water, etc.) [18,19]. GA and XG are similarly charged natural macromolecules commonly used in the food industry. Since both can undergo segregative phase separation after mixing, they were selected for investigation in this study.

While many studies have documented the effects of pH, temperature, and ionic strength on phase separation, there has been limited research on the impact of molecular weight (Mw) in this context [12,20]. In their study on the influence of polymer Mw on the phase separation of polyvinyl chloride (PVC) films, Khoryani et al. observed that lower molecular weight PVC polymers delayed delamination, while higher molecular weights favored delamination [21]. However, there is a lack of research on the influence of molecular weight on segregative phase separation in the field of food colloids. The relative Mw values are closely associated with the morphological, kinetic, and thermodynamic properties of polymer blends [22]. In this study, XG samples with different Mw were mixed with GA to obtain GA samples with varying AGP contents. This approach developed a reliable strategy for increasing the GA-derived AGP content, providing favorable influencing factors and valuable references for the potential application of segregative phase separation in the food industry.

2. Experimental section

2.1. Materials

EM10 analytical reagent powder (AR, 99 %, LOT 101008) was obtained from San Ei Gen F.F·I, Inc. (Japan). EM10 is an enhanced form of GA produced through the polymerization of AG and GP components under specific temperature and humidity conditions, resulting in a high proportion of the AGP fraction [23]. Its average Mw was 4.07×10^6 g/mol and with a polydispersity index (Mw/M_n) of 8.0. Mw measurements were conducted using a GPC-MALLS system, as previously reported [24]. XG yellow powder (AR, 99.5 %, LOT 1394) was purchased from Jungbunzlauer (Austria). The Mw of XG was 1.94×10^6 g/mol and with Mw/M_n of 2.3, as determined by gel electrophoresis, following the method described in a prior report [25]. Analytical-grade materials from Fisher Scientific and Sigma-Aldrich (UK) were used in all other instances.

Table 1
XG samples prepared for irradiation.

Sample no.	Weight (g)	State	Solvent weight (g)	Irradiation dose (kGy)	Irradiation time (h)
XG1	25.00 ± 0.06	Solid	NA	25.00	2.50
XG2	50.00 ± 0.03	5 % aqueous	47.50 ± 0.07	25.00	2.50
XG3	50.00 ± 0.05	4 % aqueous	48.00 ± 0.03	25.00	2.50
XG4	50.00 ± 0.08	3 % aqueous	48.50 ± 0.05	25.00	2.50

Note: NA, not available.

2.2. Irradiation-mediated XG degradation

XG was irradiated under an air pressure of 101.325 kPa in the solid state or various aqueous solutions. For solid-state irradiation, powdered samples were sealed in air-filled plastic tubes and irradiated using a $^{60}Co_\gamma$ source (50-k curies, 10 kGy/h, Isotron, Swindon, UK) to a dose of 25 kGy and an irradiation time of 2 h 30 min. For aqueous state irradiation, XG samples were configured with distilled water at a concentration of 3–5 %, air saturated, and irradiated at 25 kGy for 2 h 30 min [26]. Three replicate measurements were conducted for both solid and liquid irradiations. Further details regarding these samples are provided in Table 1.

2.3. Preparation of stock solutions

EM10 (40 wt%) and control XG (1 wt%) stock solutions were prepared using distilled water containing 0.005 wt% NaN_3 (as a preservative) to dissolve the corresponding powdered compounds. Similarly, the irradiated XG1 sample was prepared as XG1 (1 wt%) solution and the irradiated XG2, XG3, XG4 were diluted using distilled water containing 0.005 wt% NaN_3 to form the final XG2, XG3, XG4 (1 wt%) solutions. The solutions were stirred on a roller (LICHEN, China) for 24 h at 25 ± 1 °C to ensure full hydration, followed by storage at 4 °C. Solution concentrations are recorded as weight percentages unless otherwise stated.

2.4. Preparation of EM10/XG mixed aqueous solution

The effect of Mw on phase separation was investigated by preparing 10 g of an 8 % EM10/0.8 % XG aqueous solution (selected as the appropriate concentration for the separation region in the EM10/XG phase diagram) in centrifuge tubes. The solution was made using EM10 and XG stock solutions with different Mw values, and 0.03 g of 0.05 % direct red dye 23 was added to each tube.

2.5. Gel permeation chromatography-multiangle laser light scattering (GPC-MALLS)

The molecular characteristics of GA and the composition of the lower and upper phases after bulk phase separation at 25 °C were analyzed using a GPC-MALLS system [27]. This analysis was performed with a Superose6 10/300GL column (GE Healthcare, USA), an Agilent 1100

Table 2
The molecular parameters of control and irradiated XG samples.

Sample	Processing	Radiation dose (kGy)	Concentration (%)	Mw (10^5 g/mol)	Polydispersity (M_w/M_n)	R_g (nm)
Control XG	No irradiation	0.00	NA	19.41 ± 0.40[a]	1.37 ± 0.15[b]	119.37 ± 7.05[a]
XG1	SSI	25.00	NA	14.63 ± 0.26[b]	2.83 ± 0.25[a]	111.00 ± 5.97[a]
XG2	ASI	25.00	5.00	8.51 ± 0.35[c]	1.20 ± 0.20[b]	88.10 ± 7.10[b]
XG3	ASI	25.00	4.00	5.55 ± 0.30[d]	1.30 ± 0.20[b]	69.53 ± 5.32[c]
XG4	ASI	25.00	3.00	3.62 ± 0.30[e]	1.23 ± 0.15[b]	56.53 ± 4.47[d]

Note: Data represent the means ± standard deviation of triplicates for each measurement. Mw, weight average molecular weight; Mn, number average molecular weight; Rg, radius of gyration; NA, not available; SSI, solid-state irradiation; ASI, aqueous-state irradiation. Different lowercase letters in the same column indicate significant differences between means ($P < 0.05$).

series UV detector (Agilent Technologies, UK) set to 214 nm, a DAWN EOS multiangle light scattering detector (Wyatt Technology Corporation, USA) operating at 690 nm, and an Optilab refractometer (Wyatt Technology Corporation, UK). The eluent for these analyses was a 0.2 μm-filtered aqueous NaCl (0.2 mol/L) solution containing 0.005 % NaN_3. A KNAUER HPLC pump K-501 (Kinesis, UK) was used to maintain a flow rate of 0.4 mL/min. A 1 mL sample, with a concentration of 2 mg/mL, was injected into the GPC-MALLS system after dilution and filtration through a 0.45 μm Nylon filter. The measurements were performed in triplicate. Data collection and analysis were conducted using Astra 4.90.08 software (Wyatt Technology Corporation, USA).

2.6. Rheological analyses

A rheometer (AR 500, TA Instruments, UK) equipped with a parallel plate system (4 cm diameter) was used to assess rheological parameters, with a gap of 2000 μm. Samples were placed on the rheometer plate at the desired temperature, and any excess material was removed using a plastic spatula. Measurements were conducted at 25 °C using approximately 3 g of sample. Steady shear stress and shear rate data were collected over a shear rate range of 0.01–100 s^{-1} at 25 °C [28,29].

2.7. Statistical analysis

Each experiment was performed in triplicate. Data were analyzed using one-way analysis of variance (ANOVA), and results are presented as the mean ± standard deviation (SD). Statistical analysis was carried out using SPSS software (IBM Corp., Armonk, NY, USA), and results were considered statistically significant at $P < 0.05$.

3. Results and discussion

3.1. XG molecular parameter analyses

The molecular characteristics of XG were analyzed using the GPC-MALLS system, as described above, to assess changes in Mw due to $^{60}Co_\gamma$ irradiation and as a function of XG solution concentration. Mw values and other measurements for both control and irradiated XG samples are presented in Table 2.

The Mw values for samples XG1-XG4 ranged from 1.46×10^6 Da to 0.36×10^6 Da, while non-irradiated control XG had a Mw of 1.94×10^6 Da. Several studies have examined the effects of γ-irradiation on the viscosity and other properties of polysaccharides. For example, Kusama et al. investigated the molar masses and molar mass distributions of irradiated cellulose fibers using calibrated gel permeation chromatography. Jumel et al. employed a GPC-MALLS method to investigate the changes in Mw patterns of irradiated guar gum as a function of radiation dose [30]. In this study, the irradiated XG samples showed a significant reduction in Mw values compared to the control XG, with the extent of reduction correlating with the radiation dose and the concentration of the XG solution. In aqueous XG solutions, lower XG concentrations generated more free radicals, resulting in lower Mw values. These findings provide valuable insights for designing irradiation strategies to achieve precise control over free radical generation in aqueous solutions [31,32].

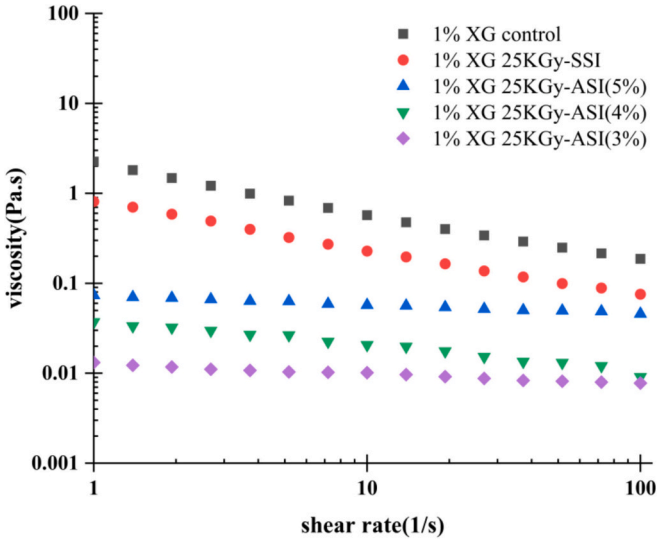

Fig. 1. Steady shear viscosity of control and irradiated XG samples in water. (All XG sample solutions had a final concentration of 1 %.)

Table 3
Steady shear viscosities of control and irradiated XG samples at 25 °C at fixed 10 s^{-1} and 50 s^{-1} shear rates.

XG samples	Steady shear viscosity at 10 s^{-1} (Pa·s)	Steady shear viscosity at 50 s^{-1} (Pa·s)
1 % XG control	1.41	0.88
1 % XG 25 kGy-SSI	0.82	0.36
1 % XG 25 kGy-ASI (5 %)	0.07	0.07
1 % XG 25 kGy-ASI (4 %)	0.04	0.03
1 % XG 25 kGy-ASI (3 %)	0.02	0.02

Shear viscosity values for control and irradiated XG preparations were analyzed (Fig. 1), revealing significant changes in rheological behavior associated with the XG state and concentration. Both control XG and solid-state irradiated XG samples exhibited shear rate-dependent viscosity, displaying flow curves characteristic of shear-thinning behavior. XG samples irradiated in aqueous solutions showed reduced viscosity dependence on shear rate due to the significant reduction in Mw. The flow curves exhibited a viscosity plateau, indicating Newtonian behavior, with shear viscosity decreasing as the aqueous solution concentrations decreased during irradiation [33,34]. Table 3 presents the shear viscosities of the control and irradiated XG samples at 10 and 50 s^{-1} shear rates, revealing a more pronounced difference in viscosity across the various XG samples. At these shear rates, both control and solid-state irradiated XG exhibited relatively high viscosity, which decreased as the concentration of the XG aqueous solution changed.

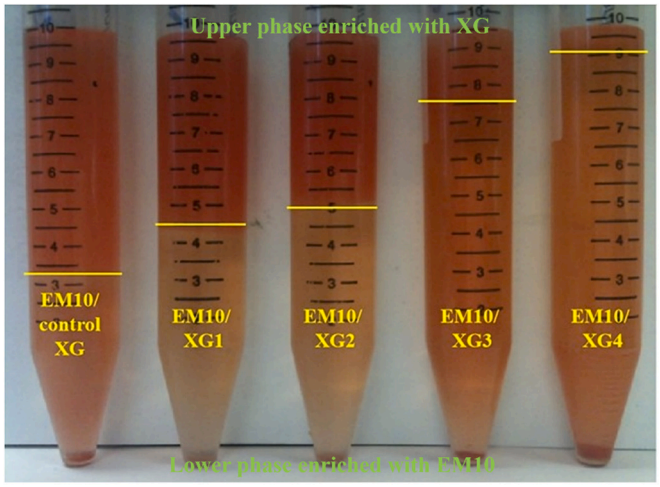

Fig. 2. Phase separation results for EM10/XG mixtures with different Mw values at a fixed concentration ratio of 8 % EM10/0.8 % XG. EM10/controlXG, EM10/XG1, EM10/XG2, EM10/XG3, and EM10/XG4 (from left to right) stained with 0.05 % Direct Red dye 23. (For interpretation of the references to color in this figure legend, the reader is referred to the web version of this article.)

However, XG samples irradiated in aqueous solutions displayed significantly lower viscosity compared to the solid-state irradiated samples, with shear viscosity decreasing as the XG concentration diminished during the preparation process.

These analyses revealed reductions in Mw, shear viscosity, and Rg values, demonstrating that the γ-irradiation of aqueous XG solutions leads to polymer degradation. This process is attributed to hydroxyl radicals generated through water radiolysis, which randomly attack the polymer chains, resulting in chain scission [35].

3.2. The impact of Mw on fractionation

Mixed solutions were prepared at final concentrations of 8 % EM10 and 0.8 % irradiated XG samples. These solutions were subjected to centrifugation for 3 h at 1788.8 ×g and 25 °C. The phase separation of EM10 and the various irradiated XG solutions is illustrated in Fig. 2.

In the mixed EM10/XG system, XG was predominantly enriched in the upper phase, while EM10 was concentrated in the lower phase, as confirmed through GPC-MALLS analysis. The figure illustrates a decrease in XG Mw values from left to right. As the Mw of XG decreased, the volume of the lower phase increased, and the boundary between the bulk phases became progressively less distinct [36]. As illustrated in Fig. 2, the volume fraction of the EM10-enriched phase increased from 32.5 % to 95 % as the XG Mw decreased. Further reductions in XG Mw to 0.55×10^6 Da and 0.36×10^6 Da (for XG3 and XG4, respectively) resulted in homogeneous phases, making it challenging to differentiate between the two phases. This behavior is attributed to the reduction in Mw, which resulted in a transition from two-phase separation to phase fusion [37,38].

Typical GPC-MALLS profile refractive index (RI) signals measured for the EM10-enriched phase from the different 8 % EM10 and 0.8 % XG sample mixtures are shown in Fig. 3. The GPC-MALLS curves display two distinct peaks: the first corresponds to the AGP peak, and the second corresponds to the AG and GP peak [12,27]. A significant increase in the AGP peak and a decrease in the AG and GP peak were evident in the EM10-enriched phase when EM10 was mixed with control XG. As the XG Mw decreased, the RI signal shape began to resemble that of control EM10, with a reduction in the AGP peak and an increase in the AG and GP peak. At a fixed concentration, the degree of EM10 fraction thus declined as the XG Mw decreased [39].

The AGP content in the EM10-enriched phase for each preparation was calculated using the GPC-MALLS software (Fig. 4). A clear decrease in AGP content in this phase was observed with declining XG Mw, decreasing from 40 % for control XG to 29 % for the XG sample with the lowest Mw. This trend aligns with the observed color changes and GPC-MALLS RI profiles. The Mw of XG appeared to influence the degree of EM10 fractionation, with a higher tendency of AGP to enter the EM10-enriched phase as the XG Mw increased. The AGP content in the EM10/control XG group was significantly higher than in the other groups ($P < 0.05$). AGP levels in the EM10-enriched phase, using the lowest Mw of XG, were similar to those for control EM10 (28.9 %) [40,41].

These results are further exemplified in Fig. 5, which shows the molar mass distributions for the EM10-enriched phases measured via GPC-MALLS. As the Mw of XG decreased from the control sample to sample XG4, the high-Mw fractions approached those in the control EM10 sample. This resulted in a reduction in the degree of AGP, AG, and GP fractionation with decreasing XG Mw, due to the weaker tendency of this system to separate into two phases. As such, a lower proportion of

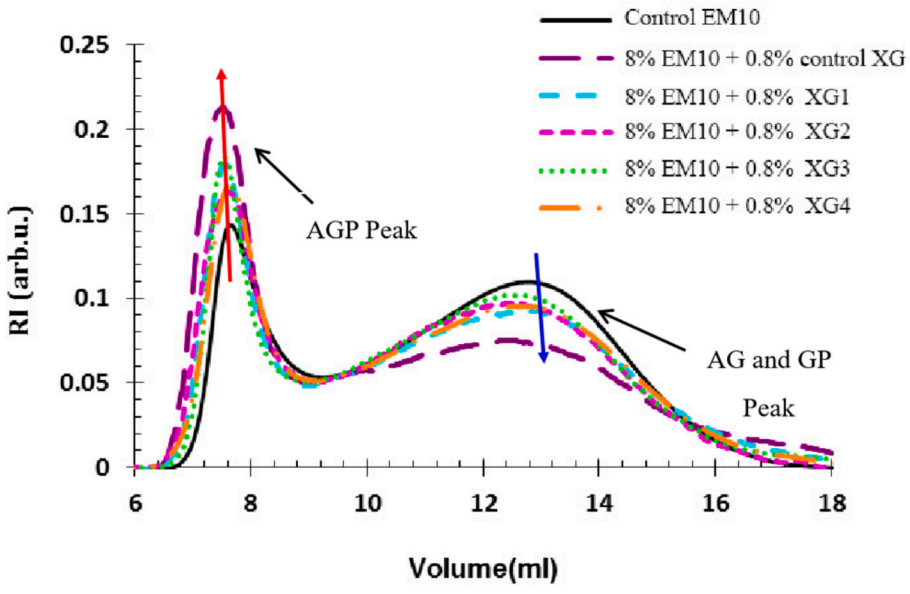

Fig. 3. GPC-MALLS RI profiles for control EM10 and various AGP-rich EM10 productions obtained from the indicated solutions.

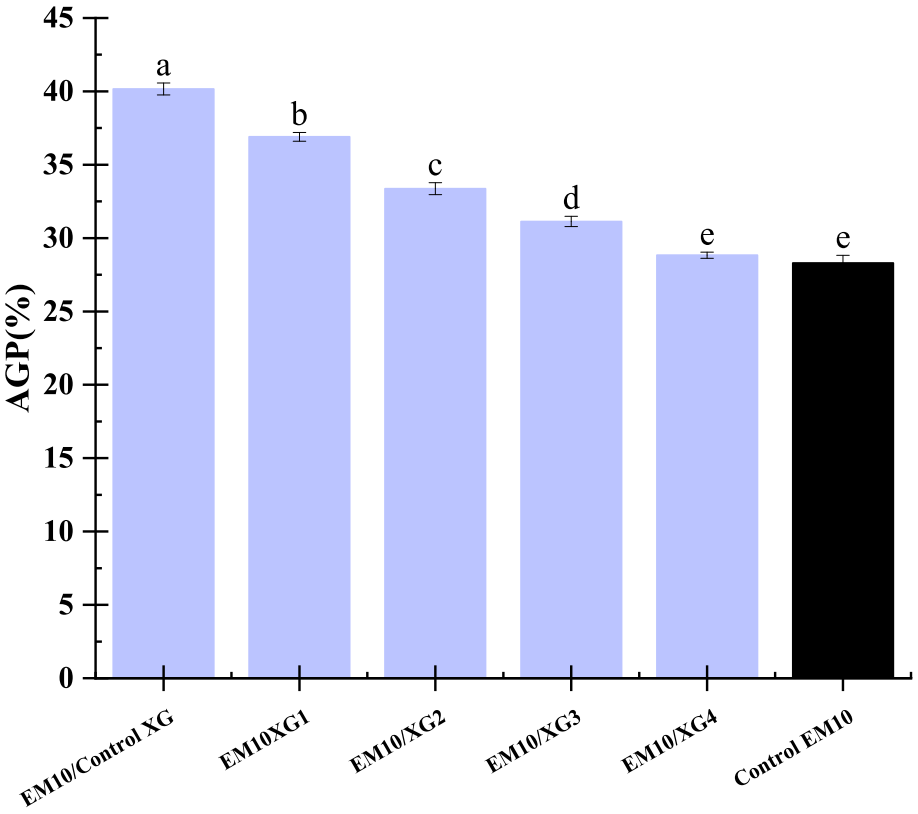

Fig. 4. AGP content levels in the EM10-enriched phase in solutions prepared with 8 % EM10/0.8 % XG mixtures of varying XG Mw values.

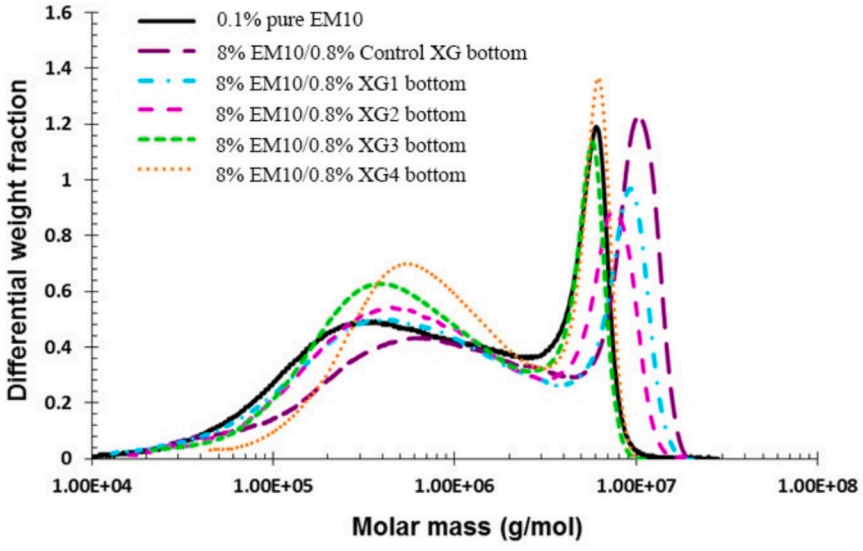

Fig. 5. Molar mass distributions of the EM10-enriched phase in mixtures of EM10 and XG with different Mw values.

AGP moved into the EM10-enriched phase as XG Mw decreased [41,42]. The Mw of the substances strongly influenced the effect of the phase separation mixture on molecular fractionation at a fixed concentration ratio. Therefore, to concentrate a functional component of one substance, increasing the Mw of the other can enhance fractionation [43]. Increasing the molecular weight of XG and mixing it with EM10 led to a higher AGP content in the EM10-enriched phase. This enhancement improved the emulsification properties of EM10, thereby increasing its potential applicability in the food industry.

4. Conclusions

Segregative phase separation has gained widespread application in the food industry, particularly in the design of functional foods and the enhancement of food properties. EM10 was found to undergo segregative phase separation, resulting in significant molecular fractionation and an increase in AGP content. This process was dependent on both the starting concentration of the mixture and the Mw of XG. When EM10 was combined with XG of varying Mw values, the degree of fractionation

decreased as Mw declined, attributed to irradiation-induced disruption of XG polymer chains. Higher Mw was found to favor more effective phase separation. These findings establish a foundation for selecting other natural polymers to explore the effects of two-phase or multi-phase segregative phase separation on their properties. This study also offers valuable insights into evaluating the influence of various factors on the molecular grading of isolated phase separation.

This study highlighted that the AGP content after mixing with GA was 29 % when the Mw of XG was a minimum of 3.6×10^5 (XG4) and 40 % when the Mw of XG was a maximum of 1.9×10^6 (Control XG). This enhancement improves the stability of GA emulsification and broadens its potential applications in food products, assuming all other influencing factors remain constant. This study only investigated the effect of Mw on segregative phase separation. Future works will explore other factors such as viscosity, mixing ratios, and macromolecular concentrations that influence segregative phase separation. In summary, the findings in this work provide new insights into the impact of Mw on the phase separation-induced fractionation of polydispersed GA/XG mixtures, along with an understanding of how irradiation methods contribute to changes in polymer Mw.

CRediT authorship contribution statement

Bing Hu: Writing – review & editing, Conceptualization. **Cunzhi Zhang:** Writing – original draft, Methodology, Investigation. **Lingyu Han:** Software, Methodology, Investigation. **Jijuan Cao:** Writing – review & editing, Methodology, Conceptualization. **Jixin Yang:** Writing – review & editing. **Qiuyue Zheng:** Validation, Software. **Xiaobo Zhang:** Validation, Software. **Yu Liu:** Methodology. **Ziang Yao:** Writing – review & editing, Methodology, Conceptualization.

Declaration of competing interest

The authors declare that they have no known competing financial interests or personal relationships that could have appeared to influence the work reported in this paper.

Acknowledgments

This article was funded by the National Natural Science Foundation of China (No. 32202232), Fundamental Research Funds for the Central Universities (04442024079), the National Key Research and Development Program (No. 2021YFF0601900), Liaoning Province Livelihood Science and Technology Project (No. 2021JH2/10200019).

Data availability

Data will be made available on request.

References

[1] B. Hu, C. Zhang, J. Zhu, J. Yang, Q. Zheng, X. Zhang, J. Cao, L. Han, Liquid−liquid biopolymers aqueous solution segregative phase separation in food: from fundamentals to applications—a review, Int. J. Biol. Macromol. 265 (2024) 131044.
[2] H. Li, Y. Liu, F. Lan, M. Ghasemi, R. Larson, Salt-dependent phase re-entry of weak polyelectrolyte complexes: from associative to segregative liquid–liquid phase separation, Macromolecules 56 (2023) 7653–8094.
[3] X. Chen, J. Xiao, J. Cai, H. Liu, Phase separation behavior in zein-gelatin composite film and its modulation effects on retention and release of multiple bioactive compounds, Food Hydrocoll. 109 (2020) 106105.
[4] B.I. Stounbjerg, Richard J. Colloids, A.P. Surfaces, E. Aspects, Associative phase separation of potato protein and anionic polysaccharides, Colloids Surf.A 566 (2019) 104–112.
[5] B.N. Molaahmadi, H. Shekarchizadeh, S.A.H.J.I.J.o.B.M.S. Goli, Function, Interactions, Segregative phase separation of gelatin and tragacanth gum solution and Mickering stabilization of their water-in-water emulsion with microgel particles prepared by complex coacervation, Int. J. Biol. Macromol. 237 (2023) 124250.
[6] I. Haug, M.A.K. Williams, L. Lundin, O. Smidsrd, K.I.J.F.H. Draget, Molecular interactions in, and rheological properties of, a mixed biopolymer system undergoing order/disorder transitions, Food Hydrocoll. 17 (4) (2003) 439–444.
[7] F. Jara, A.M.J.F.H. Pilosof, Partitioning of α-lactalbumin and β-lactoglobulin in whey protein concentrate/hydroxypropylmethylcellulose aqueous two-phase systems, Food Hydrocoll. 25 (3) (2011) 374–380.
[8] A. Matalanis, U. Lesmes, E.A. Decker, D.J.M.J.F., Fabrication and characterization of filled hydrogel particles based on sequential segregative and aggregative biopolymer phase separation, Food Hydrocoll. 24 (8) (2010) 689–701.
[9] S. Yan, P. Jiang, X. Zhang, Y. Guo, W. Fang, Cryogenic efficient phase separation of oil–water emulsions with amphiphilic hyperbranched poly(amido-amine), J. Mater. Chem. A 11 (26) (2023) 14145–14158.
[10] R. Rarima, G. Unnikrishnan, Poly(lactic acid)/gelatin foams by non-solvent induced phase separation for biomedical applications, Polym. Degrad. Stab. 177 (2020) 109187.
[11] M. Atgié, J.C. Garrigues, A. Chennevière, O. Masbernat, K. Roger, Gum Arabic in solution: composition and multi-scale structures, Food Hydrocoll. 91 (2019) 319–330.
[12] B. Hu, L. Han, Z. Gao, K. Zhang, S. Al-Assaf, K. Nishinari, G.O. Phillips, J. Yang, Y. Fang, Effects of temperature and solvent condition on phase separation induced molecular fractionation of gum arabic/hyaluronan aqueous mixtures, Int. J. Biol. Macromol. 116 (2018) 683–690.
[13] S.M.H. A, M.S. B, S.S.C. D, H.A.K.E. F, A.A. G, V.G.J.I.J.o.B.M. A, Preparation of superabsorbent eco-friendly semi-interpenetrating network based on cross-linked poly acrylic acid/xanthan gum/graphene oxide (PAA/XG/GO): characterization and dye removal ability - ScienceDirect, Int. J. Biol. Macromol. 152 (2020) 884–893.
[14] C.E. Brunchi, S. Morariu, M.J.F.h. Bercea, Impact of ethanol addition on the behaviour of xanthan gum in aqueous media, Food Hydrocoll. 120 (2021) 106928.
[15] C. Gamonpilas, C. Buathongjan, W. Sangwan, M. Rattanaprasert, P. Methacanon, Production of low molecular weight pectins via electron beam irradiation and their potential prebiotic functionality, Food Hydrocoll. 113 (2021) 106551.
[16] P.C. Srinivasa, R.N.J.F.R.I., Tharanathan, chitin/chitosan — safe, ecofriendly packaging materials with multiple potential uses, Food Rev. Int. 23 (1) (2007) 53–72.
[17] J.B. Lena, R.A. Goncalves, S.J.A.S.C. Kharel, Engineering, elucidating the effect of polyethylene terephthalate chain structure on its enzymatic degradation behavior, ACS Sustainable, Chem. Eng. 11 (38) (2023) 13974–13987.
[18] E.S. Kempner, Direct effects of ionizing radiation on macromolecules, J. Polym. Sci. Polym. Phys. 49 (12) (2011) 827–831.
[19] N.M. El-Sawy, H.A. Abd El-Rehim, A.M. Elbarbary, E.-S.A. Hegazy, Radiation-induced degradation of chitosan for possible use as a growth promoter in agricultural purposes, Carbohydr. Polym. 79 (3) (2010) 555–562.
[20] R.W. Thompson Jr., R.F. Latypov, Y. Wang, A. Lomakin, J.A. Meyer, S. Vunnum, G. B. Benedek, Evaluation of effects of pH and ionic strength on colloidal stability of IgG solutions by PEG-induced liquid-liquid phase separation, J. Chem. Phys. 145 (18) (2016) 185101.
[21] Z. Khoryani, J. Seyfi, M.J.A.S.S. Nekoei, Investigating the effects of polymer molecular weight and non-solvent content on the phase separation, surface morphology and hydrophobicity of polyvinyl chloride films, Appl. Surf. Sci. 428 (2018) 933–940.
[22] A. Geuna, M. Alvarez, A.J. Satti, Adsorbent composites of montmorillonite and chitosan of different molecular weight, obtained by gamma irradiation, J. Environ. Chem. Eng. 10 (1) (2021) 107080.
[23] L. Han, B. Hu, R. Ma, Z. Gao, KatsuyoshiPhillips Nishinari, O. Glyn, J. Yang, Y. Fang, Effect of arabinogalactan protein complex content on emulsification performance of gum arabic, Carbohydr. Polym. 224 (2019) 115170.
[24] S. Al-Assaf, G.O. Phillips, H. Aoki, Y.J.F.H. Sasaki, Characterization and properties of *Acacia senegal* (L.) Willd. var. senegal with enhanced properties (Acacia (sen) SUPER GUM (TM)): part 2 - mechanism of the maturation process, Food Hydrocoll. 21 (3) (2007) 329–337.
[25] E.M. Nsengiyumva, P. Alexandridis, Xanthan gum in aqueous solutions: fundamentals and applications, Int. J. Biol. Macromol. 216 (2022) 583–604.
[26] M. Sen, HandeTaskin, PinarTorun, MuratDemeter, MariaCutrubinis, MihalisGuven, Olgun J Radiation Physics, Chemistry, Radiation induced degradation of xanthan gum in the solid state, Radiat. Phys. Chem. 124 (2016) 225–229.
[27] P. Mao, M. Zhao, F. Zhang, Y. Fang, G.O. Phillips, K. Nishinari, F. Jiang, Phase separation induced molecular fractionation of gum arabic—sugar beet pectin systems, Carbohydr. Polym. 98 (1) (2013) 699–705.
[28] Y. Dadmohammadi, H. Torabi, S.M. Davachi, M. Childs, V. Cao, A.J. L. Abbaspourrad, Physicochemical interactions between mucin and low-calorie sweeteners: real-time characterization and rheological analyses, LWT-Food, Sci. Technol. 159 (2022) 113252.
[29] J. Li, Z. Wang, P. Wang, J. Tian, T. Liu, J. Guo, W. Zhu, M.R. Khan, H. Xiao, J. Song, On rheological properties of disc-shaped cellulose nanocrystals, Carbohydr. Polym. 330 (2024) 121764.
[30] K. Jumel, S.E. Harding, J.R. Mitchell, Effect of gamma irradiation on the macromolecular integrity of guar gum, Carbohydr. Res. 282 (2) (1996) 223–236.
[31] Hemant Dhongade, Kalyani Sakure, H. Ramchandra Badwaik, Amit Alexander, F. Tripathi Ajazuddin, Synthesis and characterisation of poly(acrylamide) grafted carboxymethyl xanthan gum copolymer, Int. J. Biol. Macromol. 85 (2016) 361–369.
[32] Y.C. A, X.D.A. B, T.L. A, M.Z. A, Q.Z. A, S.C.J.F.H. C, Effect of xanthan gum on walnut protein/xanthan gum mixtures, interfacial adsorption, and emulsion properties, Food Hydrocoll. 79 (2018) 391–398.

[33] D.D. Nguyen, R. Daneshfar, A.H.S. Dehaghani, C.H.J.J.o.M.L. Su, The effect of shear rate on aggregation and breakage of asphaltenes flocs: experimental study and model-based analysis, J. Mol. Liq. (325) (2021) 114861.
[34] M.J.C. Yamamura, A.P. Surfaces, E. Aspects, Sigmoidal temporal increase in shear viscosity of titania–toluene–ethanol colloidal suspensions, Colloid. Surface. A. 675 (2023) 132047.
[35] B. Dahlgren, C. Dispenza, M. Jonsson, Numerical simulation of the kinetics of radical decay in single-pulse high-energy electron-irradiated polymer aqueous solutions, Jpc. A 123 (24) (2019) 5043–5050.
[36] W. Jin, H. Ge, Y. Wang, X. Du, B. Li, Molecular migration of konjac glucomannan and gum Arabic phase separation and its application in oil-water interfaces, Food Hydrocoll. 61 (2016) 868–876.
[37] R. Gelles, C.W. Frank, Effect of molecular weight on polymer blend phase separation kinetics, Macromolecules 16 (9) (1983) 1448–1456.
[38] C. Cao, W. Jiang, Y. Lin, X. Chen, X.J.P.T. Chen, Sensitive phase separation behavior of ultra-high molecular weight polyethylene in polybutene, Polym. Test. 81 (2019) 106243.
[39] C. Loret, S. Schumm, P.D.A. Pudney, W.J. Frith, P.J. Fryer, Phase separation and molecular weight fractionation behaviour of maltodextrin/agarose mixtures, Food Hydrocoll. 19 (3) (2005) 557–565.
[40] M.C.A.D. Amarante, T. Maccalman, S.E. Harding, F. Spyropoulos, S. Gras, B.J.F.r.i. Wolf, Atypical phase behaviour of quinoa protein isolate in mixture with maltodextrin, Food Res. Int. 162 (2022) 112064.
[41] D.S. Tromp, M. Lankelma, H. De Valk, D.J.D.J. Emile, B.J.M. De Bruin, Aqueous phase separation behavior of highly syndiotactic, high molecular weight polymers with densely packed hydroxy-containing side groups, Macromolecules 51 (18) (2018) 7248–7256.
[42] E. Hasanvand, A. Rafe, B. Emadzadeh, Phase separation behavior of flaxseed gum and rice bran protein complex coacervates, Food Hydrocoll. 82 (2018) 412–423.
[43] S.K.Y. A, Z.E.L. B, K.C.W. A, Y.T.H. A, V.K. A, P.C.T. A, T.W.T.J.P. B, Effect of molecular weight to the structure of nanocellular foams: phase separation approach, Polymer 191 (2020) 122275.